

## Investigation of the effects of platform motion on the aerodynamics of a floating offshore wind turbine

Yuanchuan Liu<sup>1</sup>, Qing Xiao<sup>1\*</sup>, Atilla Incecik<sup>1</sup> and Decheng Wan<sup>2</sup>

<sup>1</sup>Department of Naval Architecture, Ocean and Marine Engineering, University of Strathclyde, Glasgow, UK

<sup>2</sup>State Key Laboratory of Ocean Engineering, School of Naval Architecture, Ocean and Civil Engineering, Shanghai Jiao Tong University, Shanghai, China

\*E-mail: qing.xiao@strath.ac.uk

### ABSTRACT

Along with the flourishing of the wind energy industry, floating offshore wind turbines have aroused much interest among the academia as well as enterprises. In this paper, the effects of the supporting platform motion on the aerodynamics of a floating wind turbine are studied using the open source CFD framework OpenFOAM. The platform motion responses, including surge, heave and pitch, are superimposed onto the rotation of the wind turbine. Thrust and torque on the wind turbine are compared and analysed for the cases under different platform motion patterns together with the flow field. It is shown that the movement of the supporting platform can have large influences on a floating offshore wind turbine and thus needs to be considered carefully during the design process.

**KEY WORDS:** Floating offshore wind turbine; superimposed platform motion; aerodynamics; OpenFOAM.

### INTRODUCTION

Over the last few decades, wind energy has been widely adopted as a clean and renewable energy source. According to a report published by the European Wind Energy Association<sup>[1]</sup>, the share of renewable energy in total new power capacity installations in the European Union has grown from 22.4% to 72% during 2000 and 2013. Of all 385 GW of new power capacity installations in the EU since 2000, over 28% has been wind power. While offshore wind business is growing rapidly, new generation *floating* offshore wind turbines are rapidly developed which are planned to be installed in deep water areas<sup>[2-5]</sup>. The main advantages of floating wind turbines include: the shallow water sites for fixed wind turbines are limited; wind far off the coast is even more abundant and the public concerns about visual impacts caused by onshore turbines can be minimized.

Unlike its fixed counterpart, a floating wind turbine must be supported by a floating platform which, however, further complicates the design process. The upper turbine and the lower supporting platform are

coupled/integrated in one way or another. For example, the thrust and torque acting on the turbine influences the dynamic response of a floating platform while the movement of the latter also affects the position and orientation of the turbine thus its aerodynamic performance. As far as the authors are aware, most research on the aerodynamic analysis in this area has been performed by decoupling the movement of the platform from the turbine system as a simplification. For instance, Jeon, et al.<sup>[6]</sup> adopted a vortex method to simulate a floating wind turbine undergoing a prescribed pitch motion. It was shown that when the platform moves in the upward direction to the position at a maximum velocity, thrust reaches to a maximum due to the large relative velocity. In their paper, the impacts of the pitching motion on the induced velocity were also studied. de Vaal, et al.<sup>[7]</sup> investigated a floating wind turbine with a prescribed surge motion using the BEM method with various dynamic wake models as well as the actuator disk method. Their results show that the integrated rotor loads obtained by various methods were nearly identical, indicating that the existing engineering models to deal with wake dynamics are sufficiently

accurate to cope with the additional unsteady surge motion of a wind turbine rotor in terms of its global force analysis. In the work of Tran and Kim<sup>[5]</sup> and Tran, et al.<sup>[8]</sup>, commercial CFD software packages were used to study the aerodynamic performance of a FOWT experiencing a platform pitching motion. Results were compared to those from other simplified models. Aerodynamic loads of the blade were demonstrated to change drastically with respect to the frequency and amplitude of platform pitching motion.

It is seen that most existing research has focused on a prescribed single degree of freedom (DoF) motion of the floating platform. However, from the perspective of a floating structure in reality, among the all 6DoF motion responses, surge, heave and pitch are usually present at the same time. By taking these three degrees of freedom into consideration simultaneously, a more realistic representation for the motion of platform could be made, and thus the impact of the platform motion on the aerodynamic performance of a floating wind turbine could be better illustrated.

In this paper, the open source CFD framework known as OpenFOAM<sup>[9]</sup> is adopted to study the effects of the supporting platform motion on the aerodynamics of a floating wind turbine. The platform motion responses, including surge, heave and pitch, are superimposed onto the rotation of the wind turbine.

## METHODOLOGY

In the present study, the pimpleDyMFoam solver in OpenFOAM is used which is able to solve the transient, incompressible and single-phase flow of Newtonian fluids with the moving mesh capability<sup>[9]</sup>. The incompressible Reynolds-averaged Navier-Stokes (RANS) equations with the  $k-\omega$  SST turbulence model are discretised using the Finite Volume Method (FVM). The PIMPLE (merged PISO-SIMPLE) algorithm is applied to deal with the velocity-pressure coupling in a segregated way. A second-order backward scheme is used for the temporal discretisation and a second-order upwind scheme is applied for the convective term.

OpenFOAM implements a sliding mesh technique called Arbitrary Mesh Interface (AMI) for rotating machinery problems<sup>[10]</sup>, which allows the simulation across disconnected, but adjacent, mesh domains either stationary or moving relative to one another. The AMI method is adopted in the present study to deal with the rotation of wind turbine. The prescribed surge, heave and pitch motion are applied to the whole computational domain including the rotor in such a way that the position and rotation of the turbine rotor are determined by the superimposed motion of its own

rotation and the 3DoF platform movement.

## COMPUTATIONAL MODEL

### Geometry

The NREL Phase VI wind turbine is adopted in the present study. Though this model was initially designed for the application under onshore scenarios, the availability of experimental data<sup>[11]</sup> from the National Renewable Energy Laboratory (NREL) makes it a popular validation case to verify various modelling results for aerodynamic performance of wind turbines. Given this advantage, the NREL Phase VI model is used in the present study for validation first and then as a base model for cases with prescribed platform motion.

The NREL Phase VI wind turbine is a two-bladed upwind model and each blade adopts the NREL S809 airfoil profile as shown in Fig. 1 at most of its span-wise cross sections. The length of the blade is 5.029 m from tip to the rotation axis. Of all the configurations tested by NREL, a tip pitch angle of 3 degrees is used and zero yaw angle is applied consistently in the present study. A CAD model for the wind turbine is shown in Fig. 2. The hub, nacelle and tower are not considered here for simplicity. Detailed geometry parameters can be found in the NREL report<sup>[11]</sup>.

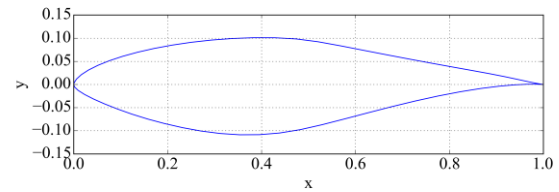


Fig. 1 Profile of NREL S809 airfoil



Fig. 2 CAD model of NREL Phase VI wind turbine

### Computational Mesh

The overall computational domain is a large cylinder shown in Fig. 3 with a diameter of  $5D$ , where  $D$  stands for the diameter of the rotor. The inlet and outlet boundaries are  $1.5D$  and  $4D$  away from the rotor, respectively. The rotor is surrounded by a small cylindrical domain and the faces connecting the two domains are defined as the AMI sliding interfaces. For a fixed wind turbine simulation, the inner small cylinder region (or rotor region) rotates about a predefined axis while the outer domain (or stator region) maintains static.

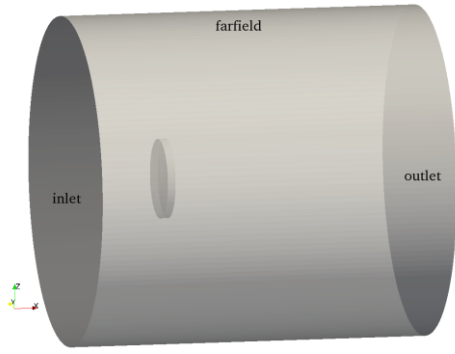


Fig. 3 Overall computational domain

The built-in snappyHexMesh utility in OpenFOAM is adopted for mesh generation. This utility is very powerful yet easy to use and capable of generating hexahedra dominant mesh <sup>[12]</sup>. An illustration of the overall computational mesh can be seen in Fig. 4. Detailed mesh near the blade is also shown in Fig. 5.

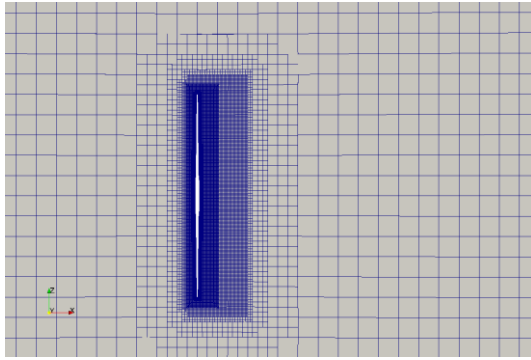


Fig. 4 Overall computational mesh

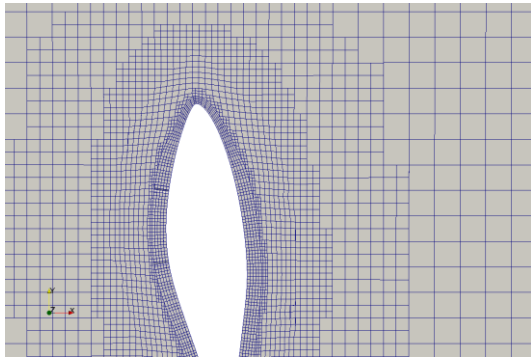


Fig. 5 Detailed mesh near blade

Since the  $k-\omega$  SST turbulence model implemented in OpenFOAM is a high-Reynolds model, wall functions are used at the rotor boundary for  $k$  and  $\omega$  variables. A spacing of 0.0035 m is applied for near wall grid cells to make sure the  $y^+$  value lies inside the interval of [30, 300]. Five layers of boundary layer cells are added near the rotor boundary to better capture the fluid flow features near the rotor. The overall computational grid size is over 10 million.

## VALIDATION

Validation is first carried out for the originally fixed wind turbine model. Four different wind velocities (5, 10, 15 and 25 m/s) are investigated and the rotational speed is fixed at 72 RPM.

### Thrust and Torque

Thrust and torque are two important aerodynamic performance parameters for a wind turbine as they represent the integrated loading on the turbine. Due to the unsteadiness caused by flow turbulence, both thrust and torque vary with time. The results presented here are obtained by averaging the time history curves over a certain period of time. A comparison between the present results and data obtained from the NREL report<sup>[11]</sup> is demonstrated in Fig. 6. The vertical bars in the figures represent the experimental standard deviation. Numerical results through CFD simulation by Li, et al.<sup>[13]</sup> are also plotted for comparison.

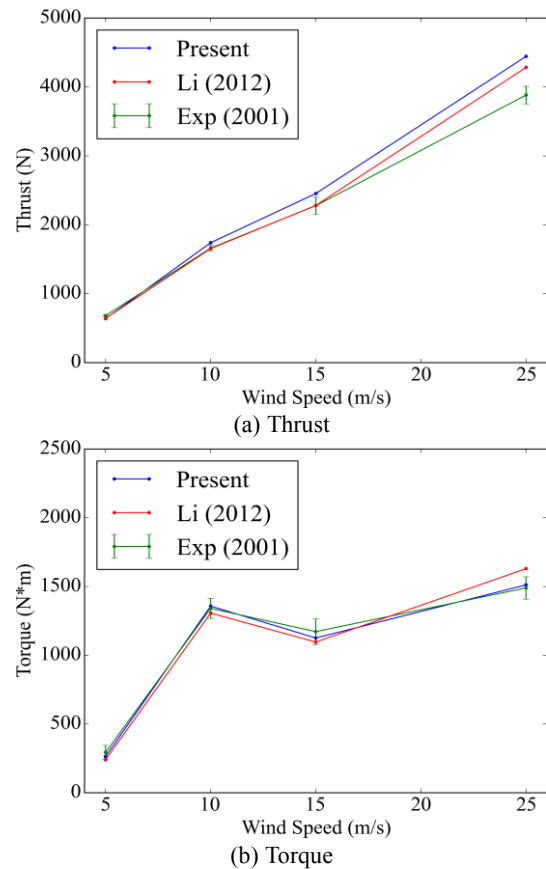


Fig. 6 Comparison of thrust and torque

As is seen from the figures, an overall good agreement has been achieved for the present results and the experimental data, indicating the validity of applying the current CFD solver to wind turbine simulation. Meanwhile, both the thrust and the torque from

present study also agree remarkably well with those from Li's paper, which further validates the modelling tool.

### Pressure Coefficients

Pressure coefficient can reflect flow information in a more detailed manner than the thrust and torque. It is defined as:

$$C_p = \frac{P_0 - P_\infty}{0.5\rho[U^2 + (\omega r)^2]} \quad (1)$$

where  $P_0$  and  $P_\infty$  are the measured pressure at a given location and the reference pressure in the far field;  $U$  stands for the wind velocity;  $\omega$  is the rotational speed and  $r$  denotes the distance between the section and rotation centre.

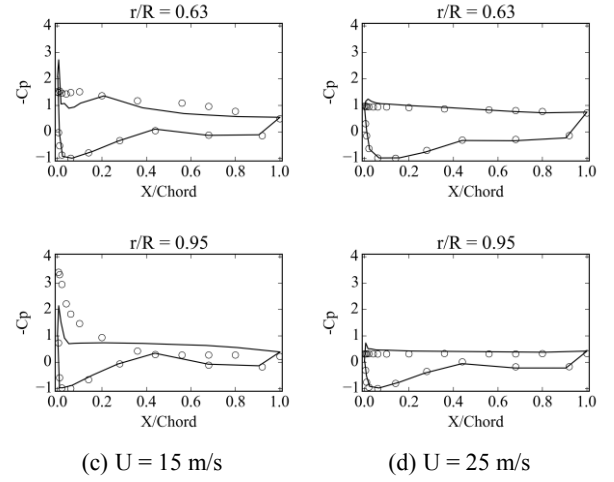
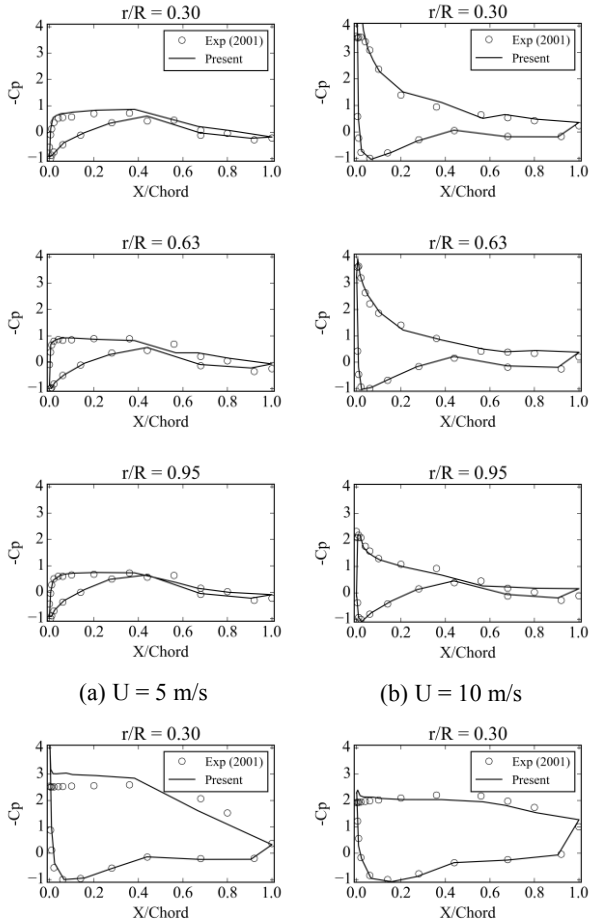


Fig. 7 Pressure coefficient for different velocities

Fig. 7 shows the comparison between predicted and measured pressure coefficients at three cross sections for four different wind velocity values. As can be seen from the figures, the predicted pressure coefficients agree quite well with the experimental data for all four wind conditions. Although some discrepancies are notable at the incoming wind velocity of 15 m/s, similar differences were also found by Li, et al.<sup>[13]</sup> and Hsu, et al.<sup>[14]</sup>.

### WORKING CONDITIONS

To investigate the effects of platform motion on the aerodynamic performance of the wind turbine, prescribed 3DoF platform motion responses (surge, heave and pitch) are superimposed in a sinusoidal form onto the rotation of the turbine rotor. Since the wind turbine was originally designed for onshore applications, assumptions are made for this offshore situation.

Offshore wind turbines usually have larger rotor diameters than onshore turbines. In the present study, the turbine under investigation is assumed to be the 1:16 scaled model of a real offshore floating wind turbine with a blade length of about 80 m. The surge, heave and pitch amplitudes are estimated based on the 1:16 scale ratio as 0.25 m, 0.1 m and 2° respectively. The centre of platform pitch motion is 6 m away in the z direction from the centre of rotation for the turbine rotor. Under regular wave conditions, the motion period for all three DoF's is the same as the incoming wave period. Four different values for the motion period are applied to investigate its influence, which are listed in Table 1. The Froude scaling law is used to determine the periods in model scale. For all cases, the wind velocity is kept as 15 m/s.

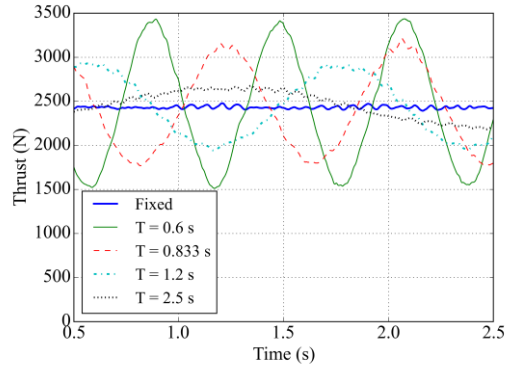
Table 1 Working conditions

Case No.	1	2	3	4
Motion Period (s)-full scale	10	4.8	3.33	2.4
Motion Period (s)-model scale	2.5	1.2	0.833	0.6

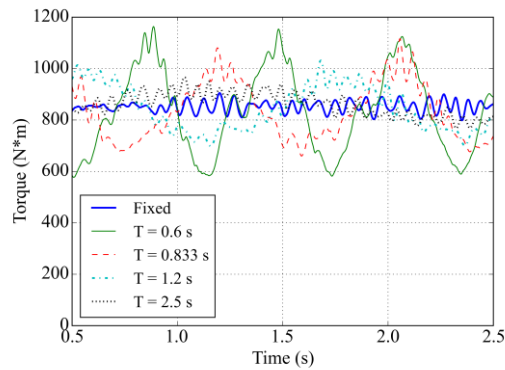
## RESULTS AND DISCUSSION

### Thrust and Torque

Fig. 8 depicts the thrust and torque time history associated with different motion periods. It is seen that both the thrust and the torque are largely affected by the superimposition of platform motion. In fact, the smaller the motion period is, the larger the amplitudes for thrust and torque are, though the time-mean values are almost the same as those under fixed conditions. Taking motion period  $T = 0.6$  s for example, the maximum thrust is almost 40% higher than the mean value while the minimum thrust is about 40% lower. Considering the large difference between the extremes, structural stress and related fatigue issue should be taken into account during the design procedure. Variation of torque may also directly influence the instantaneous power generated by the turbine.



(a) Thrust

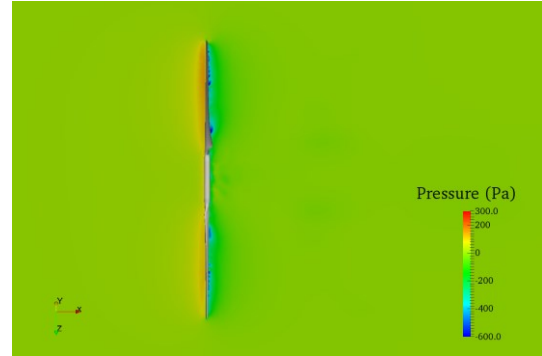


(b) Torque

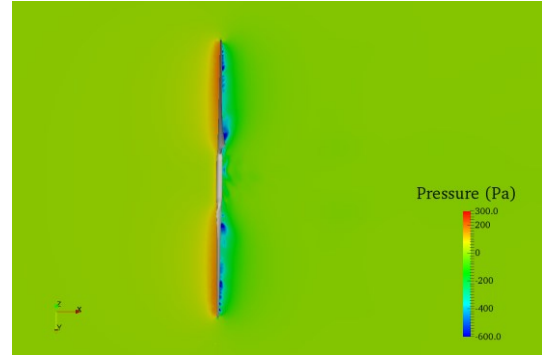
Fig. 8 Comparison of thrust and torque under various motion periods

### Flow Field

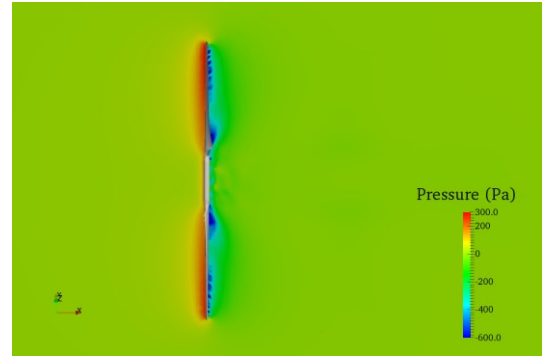
Apart from the thrust and torque, the prescribed platform motion also plays its role on the flow field around the blades and rotor. Given the time period of  $T = 1.2$  s, Fig. 9 demonstrates the pressure distribution near the turbine rotor at four time instants. A slice is cut at  $y = 0$  at the beginning and rotates along with the turbine.



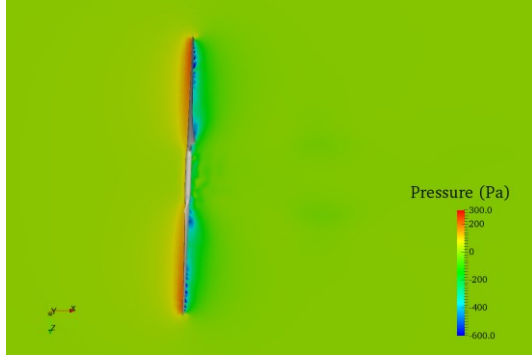
(a) Time = 1.2 s



(b) Time = 1.5 s



(c) Time = 1.8 s



(d) Time = 2.1 s

Fig. 9 Instantaneous pressure distribution near turbine rotor

Fig. 10 shows the prescribed platform motion profile. At 1.2 s, the platform is at its starting position, but velocity is at its maximum. For a surge motion, it means that the surge velocity is in the same direction as the wind velocity, thus a reduced relative wind velocity is achieved. The pressure contour displayed in Fig. 9 shows a small pressure variation before and after the rotor, corresponding to the minimum thrust in Fig. 8. At 1.5 s, although the motion is at its maximum, the velocity becomes zero just as the case without superimposed platform motion. The thrust at this instant is very close to that of a fixed wind turbine as shown in Fig. 8. The pressure difference becomes larger, so is the thrust. At 1.8 s, surge velocity reaches its maximum in the direction opposite to the wind velocity, making the relative wind velocity largest. The large pressure distribution in Fig. 9 indicates the maximum thrust in Fig. 8. Situation at 2.1 s is very similar to that at 1.5 s.

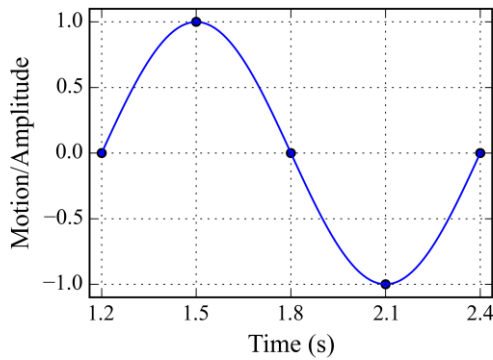
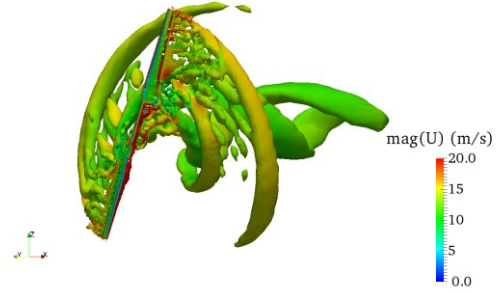


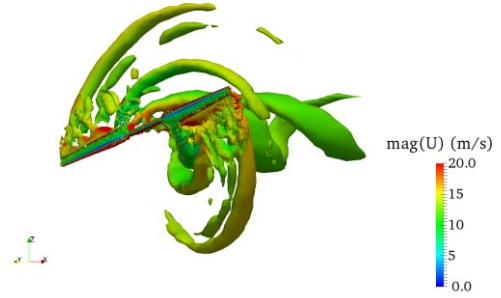
Fig. 10 Motion profile vs. time

Fig. 11 shows the vortices contours using the iso-surface of the second invariant of the rate of strain tensor ( $Q$ ) at  $Q = 5$ . Strong vortices can be seen near the blade tips as well as the blade root, where the geometry quickly changes from the NREL S809 airfoil profile to cylindrical sections. The vertical structure is also clearly influenced by the prescribed

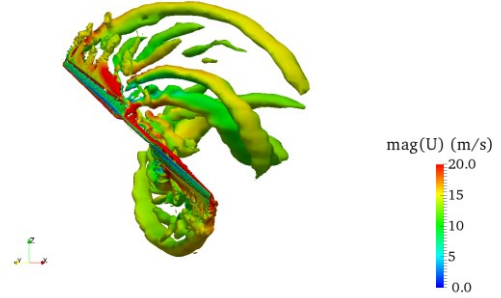
platform movement. When the turbine moves in the wind direction, it interferes with its wake, resulting in the decrease of vortices as is seen in Fig. 11 (a~b). However, when the turbine moves in the direction opposite to the wind velocity, vortices increase again as shown in Fig. 11 (c~d).



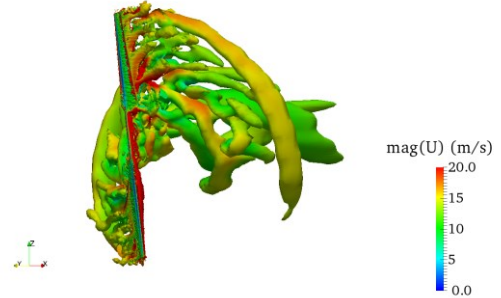
(a) Time = 1.2 s



(b) Time = 1.5 s



(c) Time = 1.8 s



(d) Time = 2.1 s

Fig. 11 Instantaneous vortices visualisation ( $Q = 5$ ) coloured by velocity magnitude



## CONCLUSIONS

In this paper, an open source CFD solver was applied to perform an aerodynamic simulation for the NREL Phase VI wind turbine model. Validation was firstly carried out against experimental test under fixed platform conditions. Numerical experimentation was later carried out by superimposing the prescribed platform 3DoF motion (surge, heave and pitch) onto the rotation of the wind turbine to simulate a floating wind turbine moving along with the supporting platform. Various motion periods were tested and aerodynamic thrust and torque of the wind turbine were analysed. It was found that both thrust and torque are largely influenced by the prescribed platform motion, indicating that the motion response of the supporting platform for a floating wind turbine should be taken into account during the design procedure. Fluid field properties such as pressure and vortices were also visualised and examined. In the next step, the interaction between the platform and waves as well as wind will be modelled so that the platform motion is directly calculated rather than prescribed to better reflect the real operating conditions.

## ACKNOWLEDGEMENT

Results were obtained using the EPSRC funded ARCHIE-WeSt High Performance Computer ([www.archie-west.ac.uk](http://www.archie-west.ac.uk)). EPSRC grant no. EP/K000586/1. This work also used the ARCHER UK National Supercomputing Service (<http://www.archer.ac.uk>).

## REFERENCES

- [1] EWEA. Wind in power: 2013 European statistics, 2014.
- [2] DeepCwind. <http://www.deepcwind.org/> (Accessed on 25 November, 2014).
- [3] FORWARD F. <http://www.fukushima-forward.jp/english/> (Accessed on 25 November, 2014).
- [4] Quallen S, Xing T, Carrica P, etc. CFD Simulation of a Floating Offshore Wind Turbine System Using a Quasi-static Crowfoot Mooring-Line Model [J], *Journal of Ocean and Wind Energy*, 2014, 1, 3, 143-152.
- [5] Tran T-T, Kim D-H. The platform pitching motion of floating offshore wind turbine: A preliminary unsteady aerodynamic analysis [J], *Journal of Wind Engineering and Industrial Aerodynamics*, 2015, 142, 65-81.
- [6] Jeon M, Lee S, Lee S. Unsteady aerodynamics of offshore floating wind turbines in platform pitching motion using vortex lattice method [J], *Renewable Energy*, 2014, 65, 207-212.
- [7] de Vaal J B, Hansen M O L, Moan T. Effect of wind turbine surge motion on rotor thrust and induced velocity [J], *Wind Energy*, 2014, 17, 1, 105-121.
- [8] Tran T, Kim D, Song J. Computational Fluid Dynamic Analysis of a Floating Offshore Wind Turbine Experiencing Platform Pitching Motion [J], *Energies*, 2014, 7, 8, 5011-5026.
- [9] OpenFOAM. The OpenFOAM website. <http://www.openfoam.com/> (Accessed on 25 November, 2014).
- [10] OpenFOAM. Arbitrary Mesh Interface (AMI). <http://www.openfoam.org/version2.1.0/ami.php> (Accessed on).
- [11] Hand M M, Simms D, Fingersh L, etc. Unsteady aerodynamics experiment phase VI: wind tunnel test configurations and available data campaigns, NREL/TP-500-29955, Golden, Colorado, USA: National Renewable Energy Laboratory, 2001.
- [12] OpenFOAM. Mesh generation with the snappyHexMesh utility. <http://www.openfoam.org/docs/user/snappyHexMesh.php#x26-1510005.4> (Accessed on).
- [13] Li Y, Paik K-J, Xing T, etc. Dynamic overset CFD simulations of wind turbine aerodynamics [J], *Renewable Energy*, 2012, 37, 1, 285-298.
- [14] Hsu M-C, Akkerman I, Bazilevs Y. Finite element simulation of wind turbine aerodynamics: validation study using NREL Phase VI experiment [J], *Wind Energy*, 2014, 17, 3, 461-481.